

Modeling the Distribution of TLS Distance-Related Uncertainties for Calibration of Geodetic Sensors

Jan Hartmann, Ingo Neumann and Hamza Alkhatib, Germany

Key words: Terrestrial Laser Scanning, Uncertainty Quantification, Probabilistic Regression, NGBoost, Sensor Calibration

SUMMARY

Accurate uncertainty quantification of terrestrial laser scanner (TLS) measurements is essential for high-precision applications such as deformation monitoring and structural health assessment. TLS distance measurements are subject to systematic deviations (μ) and measurement noise (σ), both influenced by external factors including intensity and incidence angle. Previous uncertainty modeling approaches addressed these components independently, limiting their effectiveness for rigorous quality assessment.

This research introduces a probabilistic regression framework for joint estimation of TLS distance deviation and precision using machine learning methods. The methodology employs Natural Gradient Boosting (NGBoost) and residual neural networks to predict the full Gaussian probability distribution of distance deviations, quantifying both systematic deviation and precision simultaneously. Three datasets were acquired under controlled laboratory conditions using Z+F Imager 5016 scanners with high-precision laser tracker reference measurements, enabling investigation of two critical questions: temporal stability of trained models and their transferability across different scanner units of the same type.

The results demonstrate that both models achieve RMSE values of approximately 0.50 mm with well-calibrated uncertainty intervals closely matching theoretical Gaussian coverage expectations. For same-scanner validation, systematic deviations were reduced to near-zero and standard deviations decreased from 0.70 mm to 0.52 mm. NGBoost consistently outperformed the neural network, particularly in precision prediction at low intensities, providing estimates consistent with established intensity-based reference models.

The findings reveal that distribution-based probabilistic models provide a robust methodology for TLS calibration and uncertainty quantification. Critically, calibration models for systematic deviations are scanner-specific and cannot be reliably transferred across different TLS units, whereas precision models demonstrate good transferability and temporal stability over at least one month. These advancements enhance TLS point cloud quality assessment, complementing internal scanner calibrations and facilitating uncertainty-aware decision-making in high-accuracy geodetic applications.

Modeling the Distribution of TLS Distance-Related Uncertainties for Calibration of Geodetic Sensors

Jan HARTMANN, Ingo NEUMANN and Hamza ALKHATIB, Germany

1. INTRODUCTION

Terrestrial laser scanning (TLS) has become an indispensable technology in engineering geodesy, enabling rapid acquisition of dense three-dimensional point clouds for applications ranging from deformation monitoring to structural health assessment. The reliability of TLS-derived measurements is paramount in high-precision applications where millimeter-level accuracy is required.

TLS measurements are subject to various sources of uncertainty affecting both systematic deviation and precision. While internal calibration parameters have been extensively studied (Lichti, 2010; Reshetyuk, 2009), external factors—including scan geometry and surface reflectivity—continue to pose challenges. Previous research demonstrated functional relationships between raw intensity values and measurement precision (Schill et al., 2025), while systematic deviations depend on incidence angle and surface properties (Zámečníková et al., 2014). However, existing approaches typically address these components independently.

Recent machine learning advances offer promising avenues for integrated uncertainty modeling. Hartmann and Alkhatib (2023) demonstrated effective modeling of systematic deviations using XGBoost, while Hartmann et al. (2024) achieved significant improvements through PointNet architectures incorporating spatial context. Despite these advances, a unified framework for simultaneously estimating both systematic deviation (μ) and precision (σ) remains underdeveloped.

This paper introduces a probabilistic machine learning methodology for joint modeling of TLS distance uncertainty using Natural Gradient Boosting (NGBoost) and neural networks. Our investigation addresses two research questions: (1) Is the trained uncertainty model temporally stable for the same scanner? (2) Can the model be transferred across different scanner units of the same type? Three datasets acquired under controlled conditions with Z+F Imager 5016 scanners enable systematic investigation of both temporal repeatability and inter-device variability.

2. LITERATURE REVIEW

2.1 TLS Uncertainty Sources and Modeling

TLS measurement uncertainty arises from instrumental, environmental, geometric, and object-related factors (Soudarissanane et al., 2011). Instrumental uncertainties from mechanical imperfections have been characterized through calibration procedures (Lichti, 2010), while external factors present more complex challenges. The functional relationship between raw intensity and measurement precision (Wujanz et al., 2017) has been refined through intensity-based stochastic models (Schill et al., 2025).

Hartmann and Alkhatib (2023) introduced a machine learning framework for modeling systematic TLS distance deviations, achieving $R^2 = 0.73$ using XGBoost with five features: intensity, incidence angle, distance, spot size, and curvature. Building on this, Hartmann et al. (2024) developed a modified PointNet architecture incorporating local neighborhood information, achieving approximately 16% RMSE improvement over XGBoost by capturing spatial relationships within a 5 cm radius around each point.

2.2 Probabilistic Regression for Uncertainty Quantification

The aforementioned studies focused on point estimation of systematic deviations. However, rigorous uncertainty quantification requires characterization of the full probability distribution. Probabilistic regression extends conventional approaches by predicting distribution parameters rather than point estimates (Nix and Weigend, 1994). Natural Gradient Boosting (NGBoost) (Duan et al., 2020) provides a principled framework for probabilistic prediction, offering improved stability through natural gradient descent.

2.3 Research Gap

Existing methods treat systematic bias and precision as separate quantities. The present work addresses this gap by introducing probabilistic regression models that jointly estimate both distribution parameters (μ and σ), while investigating temporal stability and cross-device transferability essential for practical implementation.

3. METHODOLOGY

3.1 Experimental Design and Data Acquisition

Three datasets were acquired under controlled laboratory conditions using Z+F Imager 5016 scanners with Leica laser trackers as reference (Table 1):

- Dataset A: Training data acquired with TLS1 (Hannover), June 2024
- Dataset B: Temporal validation with TLS1, one month earlier (May 2024)
- Dataset C: Transferability validation with TLS2 (Clausthal), simultaneous with A

Table 1: Sensor specifications.

| Sensor | Specification |
|---------------------|--|
| Leica ATS600/ATR960 | $U_3D = 15 \mu\text{m} + 6 \mu\text{m}/\text{m}$ (MPE) |
| Z+F Imager 5016 | $\sigma_d = 0.2\text{--}0.8 \text{ mm}$; $\sigma_{h,v} = 0.004^\circ$ |

Measurements were conducted in the GIH basement laboratory (controlled conditions, 20°C) with distances up to 28 m. Flat Alucore panels with varying white surface ratios (0%, 29%, 57%, 86%) served as test objects, systematically positioned at different distances and incidence angles (Figure 1).

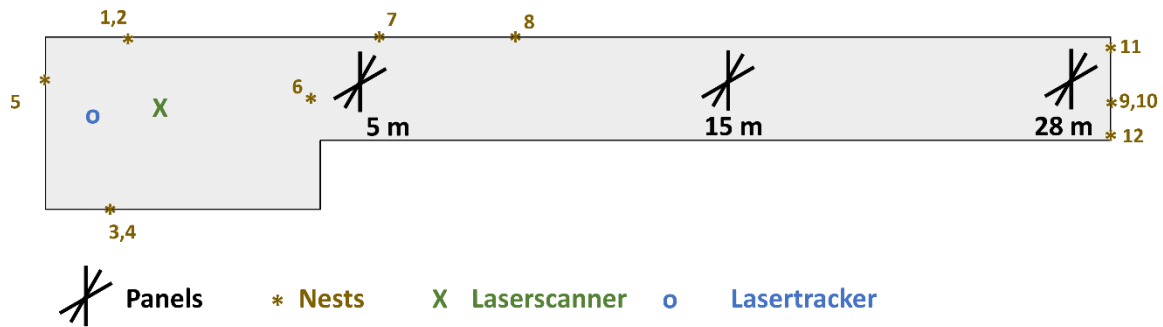


Figure 1: Experimental setup and systematic variation of measurement geometry.

3.2 Feature Extraction

Distance deviations were computed via ray casting from each TLS point to the meshed laser tracker reference surface. The distance residual $\Delta d = d_{TLS} - d_{int}$ represents the deviation between TLS measurement and reference, where positive values indicate overestimation. Three features were extracted: intensity (I_{TLS}), polar distance (d_{TLS}), and incidence angle (α).

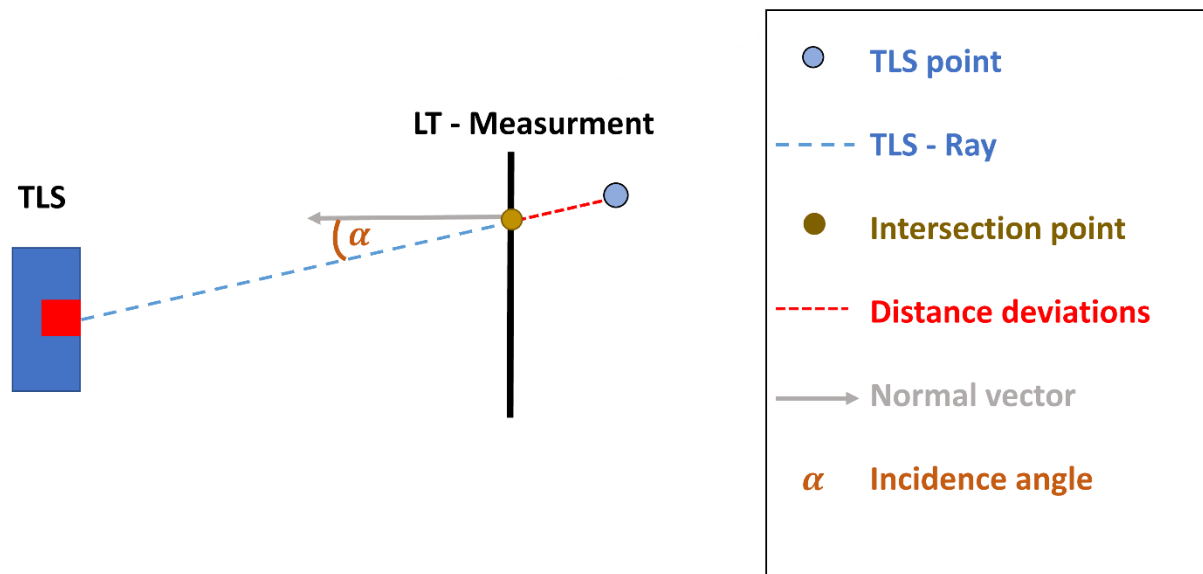


Figure 2: Ray casting methodology for feature extraction.

3.3 Probabilistic Regression Models

Both models predict Gaussian distribution parameters (μ , σ^2) using the Gaussian Negative Log-Likelihood loss:

$$\mathcal{L}_{GNLL} = \frac{1}{2} \log(2\pi\sigma^2) + (y - \mu)^2 / (2\sigma^2)$$

NGBoost (Duan et al., 2020) extends gradient boosting to probabilistic prediction using natural gradients for stable distribution parameter learning. Residual Neural Network features multiple fully connected layers with batch normalization and dropout, outputting μ and $\log(\sigma^2)$.

Hyperparameter tuning was performed on Dataset A using Bayesian optimization with 20% of the data held out for testing. Model performance was assessed using RMSE and the Continuous Ranked Probability Score (CRPS) (Gneiting and Raftery), a standard metric for comparing probabilistic forecast accuracy. The CRPS was combined with backtesting to enable more robust accuracy assessments through aggregated measurements across the dataset. Additionally, coverage analysis of predicted $k\sigma$ intervals was employed.

3.4 Software Implementation

All processing was implemented in Python using Open3D (Zhou et al., 2018) for point cloud operations, NGBoost (Duan et al., 2020), PyTorch (Paszke et al., 2019) for neural networks, and Hyperopt (Bergstra et al., 2013) for optimization.

4. RESULTS

This section presents the experimental results, beginning with statistical analysis of the distance residuals, followed by evaluation of the probabilistic models for systematic deviation prediction and precision estimation.

4.1 Statistical Analysis of Distance Residuals

4.1.1 Distribution Characteristics

Figure 3 shows the histograms of distance residuals for all three datasets. Each distribution exhibits an approximately Gaussian shape, with residuals predominantly falling within ± 2 mm.

Table 2 summarizes the descriptive statistics. All datasets show a slight positive mean, indicating that TLS distances are systematically measured too long. Datasets A and B, acquired with the same scanner at different times, exhibit comparable standard deviations (0.71 mm and 0.70 mm), while Dataset C shows lower variability (0.56 mm).

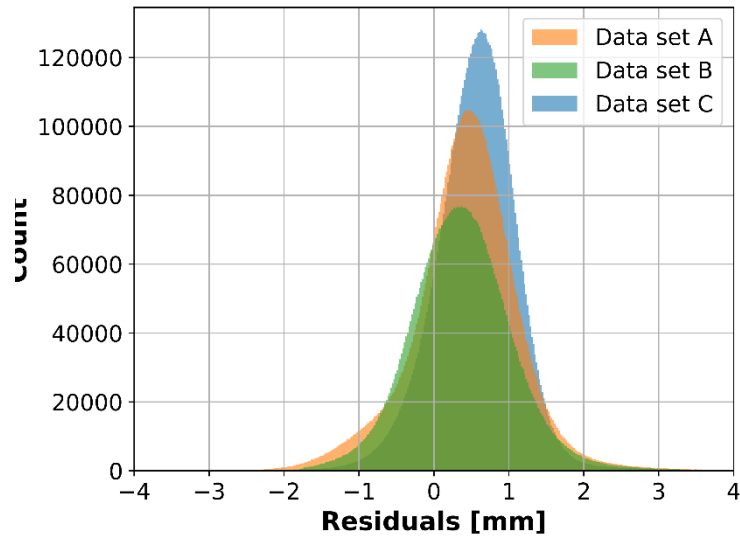


Figure 3: Distribution of distance residuals for the three datasets. All distributions approximate Gaussian shapes centered slightly above zero.

Table 2: Descriptive statistics of distance residuals for each dataset.

| Dataset | Scanner | Mean [mm] | Std. Dev. [mm] |
|--------------|------------------|-----------|----------------|
| A (Training) | TLS1 (Hannover) | 0.45 | 0.71 |
| B (Temporal) | TLS1 (Hannover) | 0.38 | 0.70 |
| C (Transfer) | TLS2 (Clausthal) | 0.56 | 0.56 |

4.1.2 Validation of Gaussian Assumption

The assumption of Gaussian-distributed residuals was validated by examining skewness and kurtosis across all measurement configurations. Figure 4 presents representative residual distributions under favorable conditions (86% white panel at 5 m) and challenging conditions (0% white panel at 28 m). Across all configurations, skewness and kurtosis values remain close to zero, confirming the validity of the Gaussian assumption for probabilistic modeling.

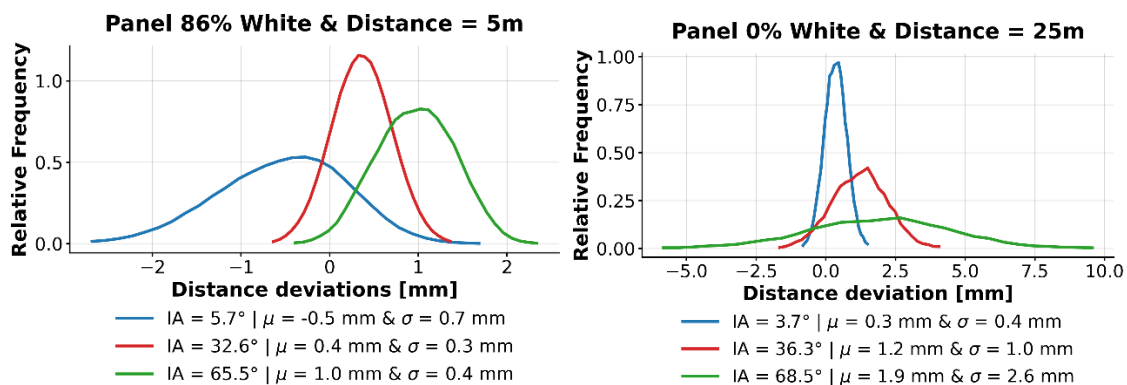


Figure 4: Validation of Gaussian distribution assumption under varying measurement conditions.

4.1.3 Feature Dependencies

Figure 5 displays hexbin plots of residuals against the three input features (intensity, incidence angle, distance) for all datasets. For Datasets A and B (same scanner), consistent patterns emerge:

- At high intensities and small incidence angles, distances are systematically underestimated by up to 1.2 mm
- At low intensities and large incidence angles, distances are overestimated by up to 1.5 mm
- Residual spread increases with decreasing intensity, increasing distance, and larger incidence angles

Dataset C exhibits notably different behavior: the systematic underestimation at high intensities is absent, and overestimation at low intensities is less pronounced. This scanner-specific variation motivates the investigation of model transferability.

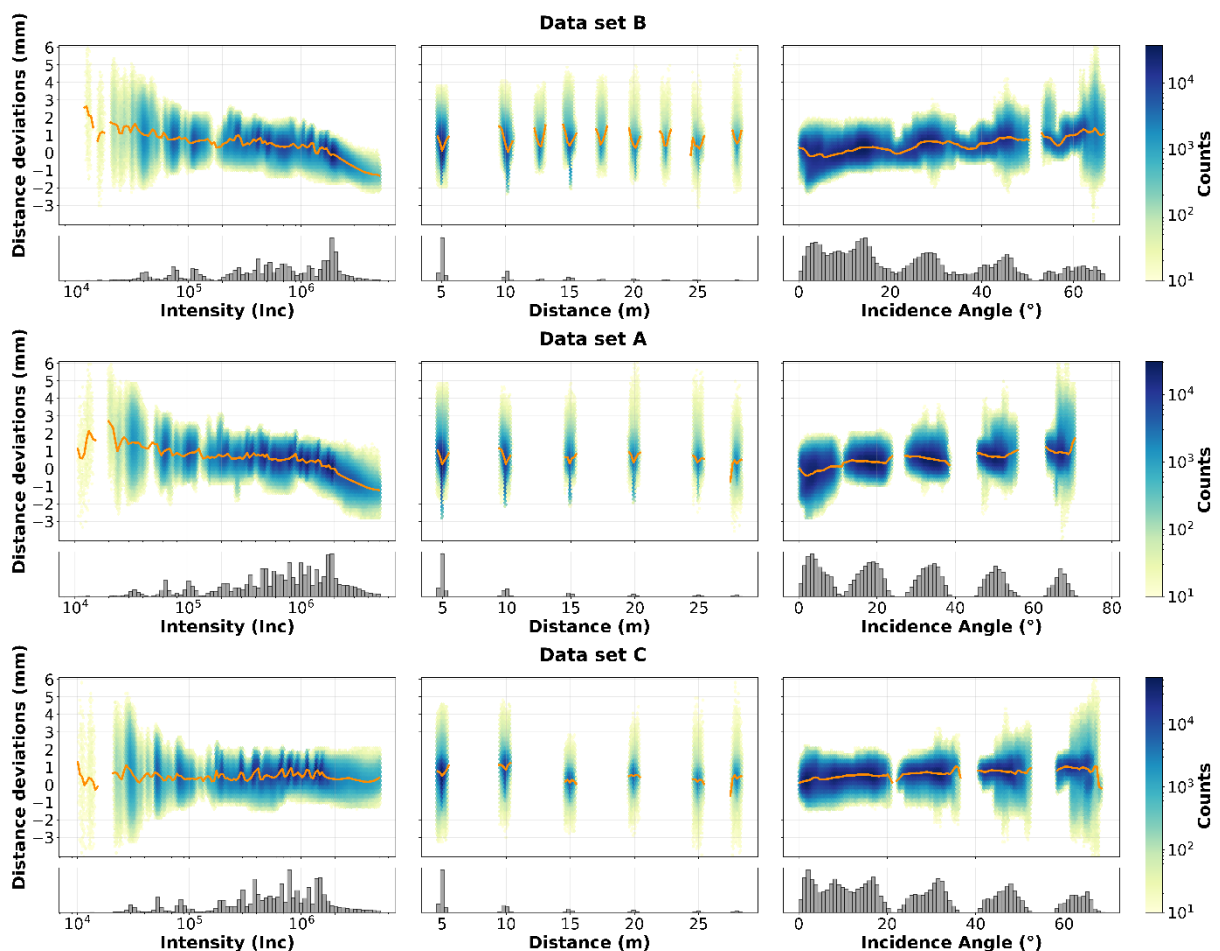


Figure 5: Residual distributions as functions of intensity, incidence angle, and distance for the three datasets.

4.2 Intensity-Based Precision Analysis

The relationship between intensity and distance precision was evaluated by fitting the parametric model $\sigma_d = a \cdot I^{b_{TLS}} + c$ to empirical standard deviations computed for each measurement configuration. Figure 6 compares the standard deviations with the reference model from the literature (Schill et al., 2025).

Datasets A and B yield nearly identical fitted curves, confirming temporal stability of precision characteristics. Dataset C shows slightly higher standard deviations at low intensities and marginally lower values at high intensities. Importantly, all empirical values exceed the reference model predictions, particularly at high intensities where the reference estimates $\sigma \approx 0.14$ mm while our measurements yield $\sigma \approx 0.25$ mm. This difference is attributed to additional uncertainty sources in our experimental setup, including TLS angular uncertainty, reference sensor uncertainty, and registration residuals.

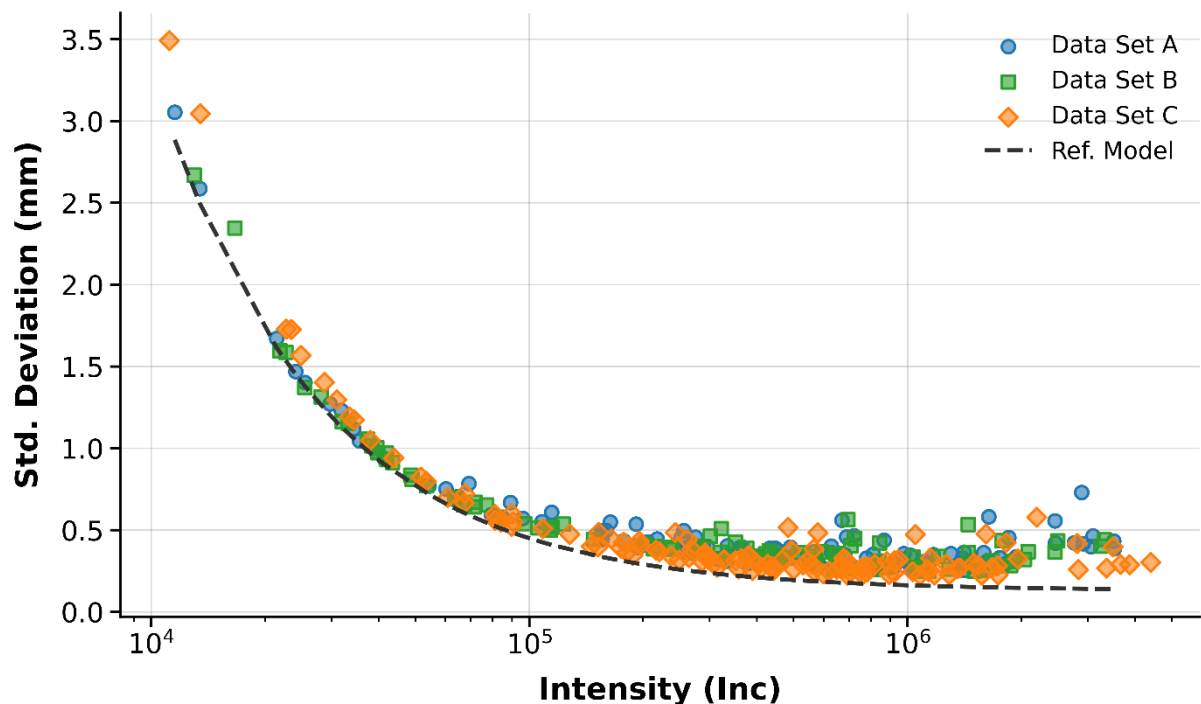


Figure 6: Empirical precision values and fitted intensity-based models for each dataset.

4.3 Probabilistic Model Evaluation

4.3.1 Systematic Deviation Prediction

Table 3 presents the evaluation metrics for systematic deviation prediction. After calibration, the mean residuals for Datasets A and B are reduced to near-zero values, with standard deviations decreasing from approximately 0.70 mm to 0.50–0.52 mm. Both models achieve comparable RMSE values of approximately 0.50 mm and CRPS values below 0.28 mm.

Table 3: Evaluation metrics for systematic deviation prediction.

| Dataset | Metric | Raw | NGBoost | Neural Net |
|--------------|---------------|------|---------|------------|
| A (Training) | μ [mm] | 0.43 | 0.00 | -0.02 |
| A (Training) | σ [mm] | 0.72 | 0.50 | 0.52 |
| A (Training) | RMSE [mm] | - | 0.50 | 0.52 |
| A (Training) | CRPS [mm] | - | 0.26 | 0.28 |
| B (Temporal) | μ [mm] | 0.38 | -0.03 | -0.13 |
| B (Temporal) | σ [mm] | 0.70 | 0.52 | 0.52 |
| B (Temporal) | RMSE [mm] | - | 0.52 | 0.53 |
| B (Temporal) | CRPS [mm] | - | 0.27 | 0.28 |
| C (Transfer) | μ [mm] | 0.56 | 0.08 | 0.02 |
| C (Transfer) | σ [mm] | 0.56 | 0.64 | 0.63 |
| C (Transfer) | RMSE [mm] | - | 0.65 | 0.63 |
| C (Transfer) | CRPS [mm] | - | 0.34 | 0.34 |

Figure 7 illustrates the effect of calibration on the residual distributions. For Datasets A and B, both models successfully center the distributions around zero. However, for Dataset C, the calibrated standard deviation increases (from 0.56 mm to 0.63–0.64 mm), indicating that applying models trained on one scanner to a different unit introduces additional uncertainty.

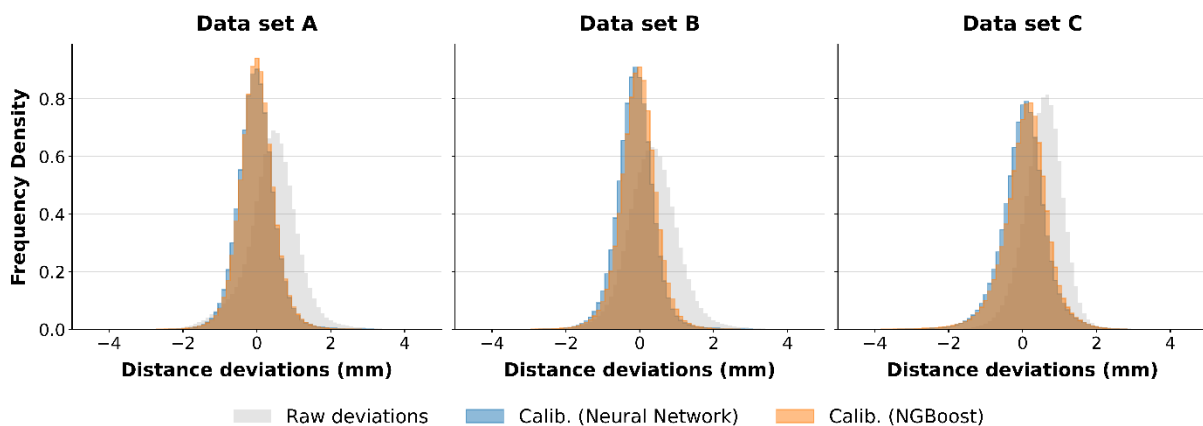


Figure 7: Residual distributions before and after calibration for each dataset.

Figure 8 shows the mean residuals as a function of intensity before and after calibration. For Datasets A and B, the systematic intensity-dependent deviations are effectively removed across most of the intensity range, with only minor residual biases at very low intensities. In contrast, calibration of Dataset C introduces new systematic effects: negative bias at low intensities and positive bias at high intensities.

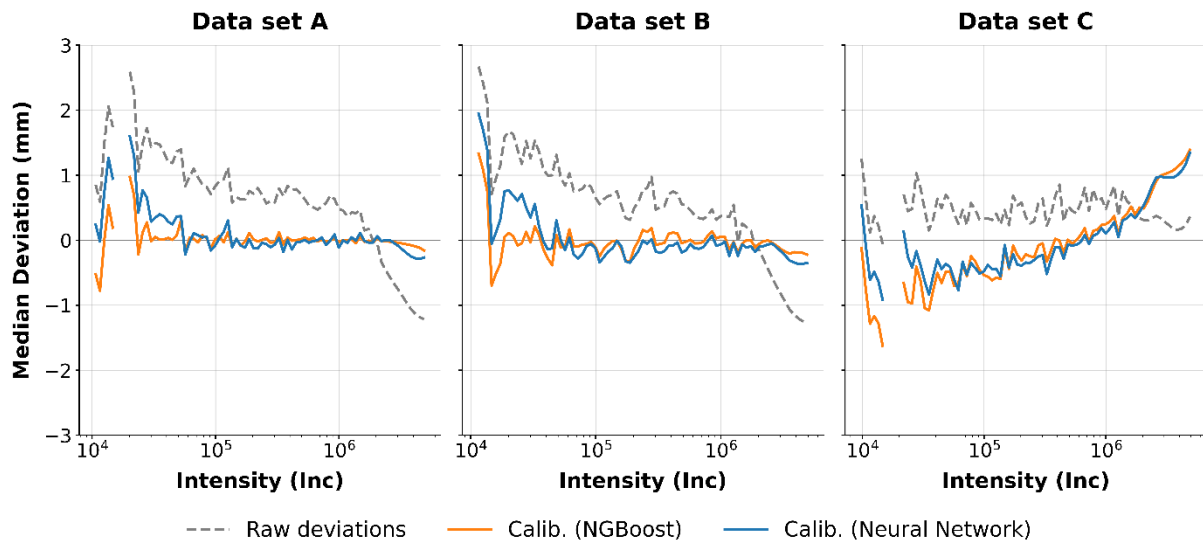


Figure 8: Effect of calibration on intensity-dependent systematic deviations.

4.3.2 Precision Prediction

The quality of predicted standard deviations was assessed through coverage analysis. Table 4 presents the empirical coverage of predicted $k\sigma$ intervals. For Datasets A and B, the coverage values closely match the theoretical Gaussian expectations (68.3%, 95.5%, 99.7%), indicating well-calibrated uncertainty estimates. Dataset C shows reduced coverage, particularly for the 1σ interval, reflecting the mismatch between trained and target scanner characteristics.

Table 4: Empirical coverage of predicted σ -intervals.

| Dataset | Interval | Theoretical | NGBoost | Neural Net |
|---------|-----------|-------------|---------|------------|
| A | 1σ | 68.3% | 68.27% | 66.34% |
| A | 2σ | 95.5% | 95.42% | 94.32% |
| A | 3σ | 99.7% | 99.80% | 99.47% |
| B | 1σ | 68.3% | 67.32% | 65.96% |
| B | 2σ | 95.5% | 94.75% | 94.05% |
| B | 3σ | 99.7% | 99.61% | 99.50% |
| C | 1σ | 68.3% | 57.49% | 60.58% |
| C | 2σ | 95.5% | 88.32% | 89.15% |
| C | 3σ | 99.7% | 97.69% | 97.39% |

Figure 9 compares predicted standard deviations against intensity for both models. NGBoost predictions align closely with the empirically fitted intensity-based model across all intensity ranges. The neural network tends to underestimate standard deviations at low intensities, likely due to data sparsity in regions with unfavorable measurement conditions. Notably, both models capture a slight increase in standard deviation at very high intensities—a pattern not represented in the analytical reference model—demonstrating the ability of data-driven approaches to reveal subtle sensor characteristics.

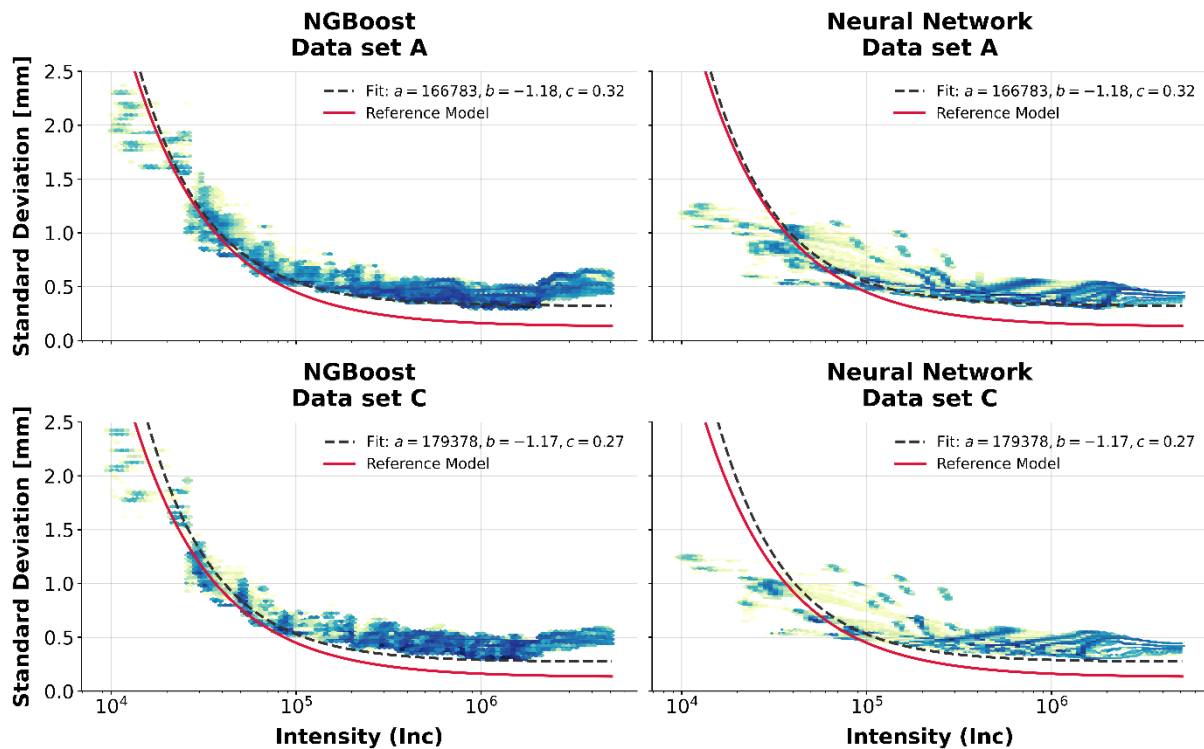


Figure 9: Comparison of predicted standard deviations with intensity-based reference model.

4.4 Model Comparison Summary

Table 5 summarizes the comparative performance of NGBoost and the neural network across both research questions.

Table 5: Summary of model performance for research questions.

| Research Question | Aspect | NGBoost | Neural Net |
|--------------------------|----------------------|-----------|------------|
| Temporal Stability (A→B) | Bias calibration | Excellent | Good |
| Temporal Stability (A→B) | Precision prediction | Excellent | Moderate |
| Transferability (A→C) | Bias calibration | Poor | Poor |
| Transferability (A→C) | Precision prediction | Excellent | Moderate |

Key findings from the model comparison:

- **Temporal stability:** Both models demonstrate excellent temporal stability when applied to data from the same scanner acquired at different times. Systematic deviations are successfully removed, and predicted uncertainties match empirical observations.
- **Sensor transferability:** Calibration models for systematic deviations are scanner-specific and cannot be reliably transferred across different TLS units of the same type. However, precision models show better transferability, with predicted standard deviations remaining plausible even for Dataset C.

– **NGBoost vs. Neural Network:** NGBoost consistently outperforms the neural network, particularly in precision prediction at low intensities. NGBoost also provides more robust calibration results for Dataset B, with smaller residual bias after correction.

5. DISCUSSION

5.1 Interpretation of Findings

The results demonstrate that probabilistic regression provides a robust framework for joint TLS uncertainty estimation. Both NGBoost and neural networks successfully learned to predict Gaussian distribution parameters, with coverage analysis confirming well-calibrated uncertainty intervals for same-scanner applications.

The excellent temporal stability between Datasets A and B has important practical implications: a single calibration campaign provides valid uncertainty models for extended periods, reducing operational burden. The consistency confirms that physical relationships between measurement conditions and distance deviations remain stable over time for a given scanner unit.

The most significant finding is the limited transferability across scanner units. Despite identical model type, TLS1 and TLS2 exhibited distinctly different systematic deviation patterns. When models trained on TLS1 were applied to TLS2, calibration introduced new biases rather than reducing uncertainty. This scanner-specificity likely arises from manufacturing tolerances, calibration history differences, and component aging effects.

5.2 Comparison with Previous Research

The methodology extends previous work (Hartmann and Alkhatib, 2023) from point estimation to full distribution modeling. While direct R^2 comparison is not applicable, achieved RMSE values (≈ 0.50 mm) approach the measurement noise floor, indicating effective capture of predictable systematic deviations.

Predicted standard deviations align well with established intensity-based models (Wujanz et al., 2017; Schill et al., 2025), though consistently exceed reference values—attributable to additional uncertainty sources (angular effects, registration, reference sensor) not considered in intensity-only models. Our estimates thus represent more comprehensive effective uncertainty for practical applications.

An unexpected benefit is the ability to reveal sensor behaviors not captured by analytical models, including the σ increase at very high intensities, suggesting detector saturation effects.

5.3 Asymmetric Transferability

While systematic deviation predictions failed to generalize across scanners, precision predictions maintained reasonable accuracy even for Dataset C. This asymmetry reflects different physical origins: precision derives from fundamental noise processes similar across units, while systematic deviations arise from unit-specific optical and electronic interactions.

5.4 Limitations and Practical Recommendations

Several limitations of this study should be acknowledged. First, all training data were acquired on planar surfaces with homogeneous reflectivity properties. Real-world applications involve

complex geometries including edges, corners, and curved surfaces where local neighborhood effects may significantly influence measurement quality. Second, the maximum measurement range of 28 m, while representative of many indoor applications, limits direct applicability to long-range scanning scenarios common in topographic surveys. Third, the controlled laboratory environment (constant temperature, humidity, and lighting) does not capture environmental variability encountered in field conditions. Fourth, our investigation focused on a single scanner model (Z+F Imager 5016); generalization to other manufacturers and scanner types requires additional validation.

The feature set employed—intensity, distance, and incidence angle—represents readily available point attributes but excludes potentially informative variables such as surface roughness, ambient light conditions, and temporal variations within a single scan. Incorporating these additional features may further improve model performance but requires more sophisticated data acquisition protocols.

For practitioners seeking to implement this methodology, we offer the following recommendations:

- 1. Scanner-specific calibration is essential:** Each TLS unit requires individual characterization for systematic deviation correction. Models trained on one scanner cannot be reliably transferred to another unit, even of identical type. Organizations operating multiple scanners should plan for individual calibration campaigns.
- 2. Precision models offer broader applicability:** Unlike systematic deviation models, precision predictions demonstrate reasonable transferability across scanner units. When scanner-specific calibration is impractical, precision models from similar scanner types may still provide useful uncertainty estimates.
- 3. NGBoost is recommended over neural networks:** For this application domain, NGBoost consistently demonstrated superior performance, particularly in data-sparse regions typical of challenging measurement conditions. Additionally, NGBoost offers faster training times and requires less hyperparameter tuning than neural network alternatives.
- 4. Temporal stability supports extended deployment:** The demonstrated one-month stability suggests that calibration models remain valid over extended periods without frequent recalibration. However, we recommend periodic validation—particularly after significant scanner maintenance, firmware updates, or mechanical impacts.
- 5. Integration with existing workflows:** The probabilistic predictions can be directly integrated into downstream processing chains, enabling point-wise uncertainty propagation through surface reconstruction, deformation analysis, or change detection algorithms.

6. CONCLUSIONS

This paper presented a probabilistic machine learning framework for joint modeling of TLS distance uncertainty, enabling simultaneous estimation of systematic deviations (μ) and precision (σ). The methodology was validated using three datasets acquired with Z+F Imager 5016 scanners under controlled conditions.

6.1 Main Findings

1. Feasibility of distribution-based modeling: Both NGBoost and neural networks successfully predict Gaussian distance deviation distributions, achieving RMSE ≈ 0.50 mm and well-calibrated uncertainty intervals matching theoretical coverage expectations.
2. Temporal stability confirmed: Calibration models demonstrate excellent stability when applied to the same scanner at different times, enabling extended validity periods without frequent recalibration.
3. Limited cross-scanner transferability: Systematic deviation models are scanner-specific and cannot be transferred across units. However, precision predictions show better transferability, providing useful uncertainty estimates even without unit-specific training.

NGBoost consistently outperformed neural networks, particularly for precision prediction in data-sparse regions, and is recommended for this application domain.

6.2 Future Work

The findings of this study open several promising avenues for future research. A natural first extension involves adapting the methodology to handle complex geometries beyond the planar surfaces employed in this investigation. Real-world scanning scenarios frequently encounter edges, corners, cylindrical structures, and irregular surfaces where mixed-pixel effects and geometric discontinuities introduce additional uncertainty sources not captured by the current framework. Addressing these challenges requires development of appropriate reference measurement strategies for non-planar geometries and modified feature extraction approaches that account for local surface curvature.

A particularly promising direction involves integrating the probabilistic regression framework with deep learning architectures that leverage spatial context. Combining the PointNet-based approach of Hartmann et al. (2024) with the distribution-based uncertainty quantification presented here could yield hybrid architectures that simultaneously capture spatially-correlated error patterns while providing well-calibrated uncertainty intervals. This integration presents technical challenges but offers significant potential for capturing complex spatial dependencies.

Transitioning to practical validation, systematic evaluation under varying environmental conditions represents a critical step toward operational deployment. The controlled laboratory environment employed in this study does not capture the variability encountered in field applications, including temperature gradients, humidity variations, and mixed lighting conditions. Furthermore, extending the validated measurement range beyond 28 m would broaden applicability to topographic surveys and infrastructure monitoring applications requiring distances of 50–300 m, where atmospheric effects and reduced signal-to-noise ratios present additional challenges.

Finally, exploring multi-scanner ensemble approaches offers possibilities for improving generalizability. Training precision models on pooled data from multiple scanner units might capture common underlying noise physics while averaging out unit-specific characteristics, providing more robust uncertainty estimates without extensive individual calibration.

6.3 Concluding Remarks

Distribution-based probabilistic modeling provides a robust methodology for TLS uncertainty quantification. The demonstrated temporal stability supports practical deployment, while

scanner-specificity of systematic deviations emphasizes the need for individual unit characterization. This methodology advances TLS quality assessment, serving as a complement to manufacturer calibrations and enabling uncertainty-aware decision-making in high-accuracy geodetic applications.

REFERENCES

- Bergstra, J., Yamins, D., and Cox, D. D. (2013). Making a science of model search: Hyperparameter optimization in hundreds of dimensions for vision architectures. In *Proceedings of the 30th International Conference on Machine Learning (ICML)*, pages 115–123.
- Duan, T., Avati, A., Ding, D. Y., Thai, K. K., Basu, S., Ng, A. Y., and Schuler, A. (2020). NGBoost: Natural gradient boosting for probabilistic prediction. In *Proceedings of the 37th International Conference on Machine Learning (ICML)*, pages 2690–2700.
- Gneiting, T. and Raftery, A. E. (2004). Strictly proper scoring rules, prediction, and estimation. Technical Report no. 463, Department of Statistics, University of Washington, Seattle, Washington, USA
- Hartmann, J., Ernst, D., Neumann, I., and Alkhatib, H. (2024). PointNet-based modeling of systematic distance deviations for improved TLS accuracy. *Journal of Applied Geodesy*, 18(4):613–628.
- Hartmann, J. M. and Alkhatib, H. (2023). Uncertainty modelling of laser scanning point clouds using machine-learning methods. *Remote Sensing*, 15(9):2349.
- Lichti, D. D. (2010). Terrestrial laser scanner self-calibration: Correlation sources and their mitigation. *ISPRS Journal of Photogrammetry and Remote Sensing*, 65(1):93–102.
- Nix, D. A. and Weigend, A. S. (1994). Estimating the mean and variance of the target probability distribution. *Proceedings of 1994 IEEE International Conference on Neural Networks*, 1:55–60.
- Paszke, A., Gross, S., Massa, F., et al. (2019). PyTorch: An imperative style, high-performance deep learning library. *Advances in Neural Information Processing Systems*, 32:8024–8035.
- Reshetyuk, Y. (2009). Self-calibration and direct georeferencing in terrestrial laser scanning. PhD thesis, Royal Institute of Technology (KTH), Stockholm, Sweden.
- Schill, F., Holst, C., Wujanz, D., Hartmann, J., and Paffenholz, J.-A. (2025). Intensity-based stochastic model of terrestrial laser scanners: Methodological workflow, empirical derivation and practical benefit. *ISPRS Open Journal of Photogrammetry and Remote Sensing*, 15:100079.
- Soudarissanane, S., Lindenbergh, R., Menenti, M., and Teunissen, P. (2011). Scanning geometry: Influencing factor on the quality of terrestrial laser scanning points. *ISPRS Journal of Photogrammetry and Remote Sensing*, 66(4):389–399.
- Wujanz, D., Burger, M., Mettenleiter, M., and Neitzel, F. (2017). An intensity-based stochastic model for terrestrial laser scanners. *ISPRS Journal of Photogrammetry and Remote Sensing*, 125:146–155.
- Zámečníková, M., Wieser, A., Woschitz, H., and Ressel, C. (2014). Influence of surface reflectivity on reflectorless electronic distance measurement and terrestrial laser scanning. *Journal of Applied Geodesy*, 8(4):311–326.
- Zhou, Q.-Y., Park, J., and Koltun, V. (2018). Open3D: A modern library for 3D data processing. arXiv preprint arXiv:1801.09847.

BIOGRAPHICAL NOTES

Jan HARTMANN is a PhD candidate at the Geodetic Institute of Leibniz Universität Hannover since 2021. His research focuses on TLS uncertainty modeling using machine learning methods.

Prof. Dr.-Ing. Ingo NEUMANN is Full Professor and Managing Director at the Geodetic Institute of Leibniz Universität Hannover since 2012/2015. His PhD (2009) addressed uncertainty modeling in parameter estimation. Research interests include engineering geodesy and geodetic data analysis.

PD Dr.-Ing. habil. Hamza ALKHATIB is Professor at the Geodetic Institute of Leibniz Universität Hannover. His PhD (Bonn, 2007) covered Monte Carlo methods for satellite gravity missions; habilitation (2020) addressed computational geodetic data analysis. Research focuses on Bayesian modeling, uncertainty quantification, and sensor fusion.

CONTACTS

M.Sc. Jan HARTMANN
Leibniz Universität Hannover, Geodetic Institute
Nienburger Str. 1
30167 Hannover, GERMANY
Tel. +49 511 762 12311
Email: hartmann@gih.uni-hannover.de
Web site: <https://www.gih.uni-hannover.de/de/janhartmann>

Prof. Dr.-Ing. Ingo NEUMANN
Leibniz Universität Hannover, Geodetic Institute
Nienburger Str. 1
30167 Hannover, GERMANY
Tel. +49 511 762 2461
Email: neumann@gih.uni-hannover.de
Web site: <https://www.gih.uni-hannover.de/de/neumann>

PD. Dr.-Ing. Hamza ALKHATIB
Leibniz Universität Hannover, Geodetic Institute
Nienburger Str. 1
30167 Hannover, GERMANY
Tel. +49 511 762 2464
Email: alkhatib@gih.uni-hannover.de
Web site: <https://www.gih.uni-hannover.de/de/alkhatib>